Fitness costs of adaptive chlorantraniliprole resistance in the *Spodoptera exigua* (Lepidoptera: Noctuidae)

Abstract

The beet armyworm, *Spodoptera exigua*, is a multifeeding insect pest, which has developed high resistance to chlorantraniliprole, a benzoylurea insecticide that targets on the ryanodine receptors (RyRs). However, few studies have been conducted on the highly resistant strain. Here, the resistant strain (SE-Sel) and sensitive strain (SE-Sus) were obtained by bidirectional screening for 6 generations. The potential oviposition and oviposition rate of the SE-Sel strain were dramatically lower than those of the SE-Sus strain, on the contrary the weights of prepupae and preadult were significantly increased. And the expression levels of *vitellogenin* (*SeVg*) and its receptor (*SeVgR*) in the SE-Sel strain were consistently lower than those in the SE-Sus strain. The RyR^{I4765M} mutation and the upregulation of detoxification genes, such as *SeABCOK*, *SeGST15*, *SeGSTZ2*, *SeCarEs1*, *CYP6AEW* and *SeCYP6AB10*, contributed to the evolution of resistance to chlorantraniliprole. The RyR^{I4765M} mutation could affect neuropeptide activation, and it conduced to the upregulated expression of the neuropeptide *SeNPF* and its receptor, *SeNPFR*, which could inhibit courtship behavior and reduce oviposition. And the neuropeptide *SeNPF* could influence the expression of *juvenile hormone-binding protein* and *juvenile hormone diol kinase*, and it led to the downregulated expression of *SeVg*. Therefore, these results indicate that the fitness cost accompanied by chlorantraniliprole resistance in *S. exigua* is related to the wicked evolution of RyR.

KEYWORDS: Spodoptera exigua, Chlorantraniliprole, Vitellogenin, Fitness Cost, Ryanodine Receptor Mutation

1 | INTRODUCTION

The beet armyworm, *Spodoptera exigua* Hübner, an important insect pest that threatens numerous cash crops, such as *Zea mays*, *Nicotiana tabacum*, and *Medicago sativa*, survives wintering by migration without diapause and causes economic losses worldwide (Moulton et al., 2002; Wu et al., 2010; Zhou et al., 2011; Zheng et al., 2012). Chemical insecticides have been the most effective means of controlling this pest for the last two decades, including some traditional organophosphorus, pyrethroid, and benzoylurea insecticides and other supplemented newer insecticides in recent years (Lai et al., 2011; Che et al., 2013; Su et al., 2014; Zhang et al., 2014).

Chlorantraniliprole is a novel benzoylurea insecticide that targets on the ryanodine receptors (RyRs), which are ion channels that regulate intracellular Ca^{2+} release during physiological excitation-contraction coupling (Truong et al., 2019), leads to the overrelease of internal calcium ion (Ca^{2+}) stores, and subsequently causes feeding cessation, muscle paralysis and ultimately death (Teixeira et al., 2013; Sun et al., 2015), and the overrelease of Ca^{2+} also enhances neuropeptide activation to regulate ovarian development (James et al., 2014; McKinney et al., 2016; Truong et al., 2019). It is effective against almost all lepidopterist pests and is safe for mammals, birds, and fishes (Lahm et al., 2007; David et al., 2008). However, owing to the overuse of this insecticide, field populations collected from different districts in China have evolved to a high level of resistance to chlorantraniliprole (Lai et al., 2011; Gao et al., 2013). In 2012, 16 populations of *S. exigua* in seven provinces in China were monitored on the resistance levels, with resistance ratios (RR) of 2-44-fold to chlorantraniliprole (Che et al., 2013). In recent years, Guo et al. (2014a) also declared that their group has found a field-resistant population of *Plutella xylostella* with 2,128 RR to chlorantraniliprole in Yunnan Province. Wang et al. (2015) reported that the resistance of *P. xylostella* to chlorantraniliprole in Guangdong Province had reached 2,000-fold. Wang et al. (2018b) found that the resistances of *S. exigua* collected in 2016 were significantly higher than two years earlier, especial for chlorantraniliprole with RRs rising from 173.4- to 582.6-fold.

Normally, the evolution of resistance to an insecticide is accompanied by a high expensive cost or striking weaknesses that could diminish the insect's fitness in comparison to its susceptible counterparts in the population (Kliot et al., 2012; Abbas et al., 2016), especially for reproduction fitness costs; for example, resistant insects have lower fertility and longer developmental duration

than sensitive insects, which is not conducive to insect population growth. Cao and Han (2010) found that the mating rate and hatching rate of tebufenozide-resistant *P. xylostella* strain were significantly reduced. Ribeiro et al. (2013) found that the chlorantraniliprole-resistant strain of *P. xylostella* presented significantly lower fecundity and higher larval and pupal periods, hatchability, and male longevity compared with the susceptible strain. Abbas et al. (2014) also found that profenofos-resistant strain of *Spodoptera litura* have reduced fertility and hatching rates and lower intrinsic growth rates. The resistant strain has shown an adaptive cost in comparison to the susceptible strain that could result in a delay in population growth in the field (Passos et al., 2019).

Vitellogenin (Vg) is an indispensable reproduction-related protein that is traditionally identified as an appropriate parameter for appraising female fertility in insects (Ma et al., 2019). In most insects, Vg is mainly synthesized by fat bodies or other tissues, for example ovarian tissues (Wahli, 1988), secreted to the hemolymph, binds to the vitellogenin receptor and finally enters the cell through endocytosis after reaching at the oocyte surface (Giorgi et al., 1999; Tufail et al., 2014). In our laboratory, a resistant strain (SE-Sel) of *S. exigua* was established through continuous selection with the sublethal dose of chlorantraniliprole. However, the resistance mechanism and fitness cost accompanied by the insecticide were still not clearly. Identifying the fitness cost and the dominance of the fitness cost accompanied by insecticide resistance could be useful for designing an integrated pest management (IPM) program that limits the rapid propagation of the resistant population (Abbas et al., 2016). Therefore, in the current study, a comparison of the ability and gonad coefficiency between the SE-Sel and sensitive strains (SE-Sus) was employed to investigate whether the fitness cost was accompanied with chlorantraniliprole resistance in *S. exigua*. In addition, transcriptome analysis of the SE-Sel and SE-Sus strains, and reproduction-related genes was performed to investigate the underlying mechanism. The results of the present study can be useful in designing appropriate management strategies for resistant insect populations.

2 | METHODS

2.1 | Insects

The resistance ratios for the SE-Sus and SE-Sel strains (with LC_{50} values of 0.502 µg/g and 5.837 µg/g respectively) were estimated at 3.72- and 226.69-fold, compared with the LC_{50} value of 0.061

81 μg/g in Sus-Lab to chlorantraniliprole. All stages were maintained under the same standard

82 conditions of 27 ± 1 °C, 70–80% RH, and a 16:8 h (L:D) photoperiod. The larvae and adults were

83 reared with an artificial diet and a 10% sugar solution, respectively. Pupae and newly laid eggs were

84 sterilized with a 0.2–0.3% sodium hypochlorite disinfectant solution (Wang et al., 2018b). The

85 susceptible strain (Sus-Lab) of *S. exigua* was alimented in the laboratory without exposure to any

86 insecticide since 2003. Leshan's population from the original field samples was collected in 2017

87 from vegetable fields in the Mouzi town of Leshan City in Sichuan Province, China. The SE-Sus

88 strain was established from the untreated offspring of pairs in the Leshan population with the

89 highest mortality by continual selection with gradually increasing concentrations of

90 chlorantraniliprole, on account of the LC_{70} values from the bioassay of their parent generations for a

91 total of 6 generations; In contrast, SE-Sel was screened by treating the offspring of pairs with

92 gradually diminishing concentrations of chlorantraniliprole, on account of the LC_{30} values for a

93 total of 6 generations, according to the method described by Huang et al. (2019). The resistance

94 ratios for the SE-Sus and SE-Sel strains (with LC_{50} values of 0.502 μg/g and 5.837 μg/g respectively)

95 were estimated at 3.72- and 226.69-fold, compared with the LC_{50} value of 0.061 μg/g in Sus-Lab to

96 chlorantraniliprole. All stages were maintained under the same standard conditions of 27 ± 1 °C,

97 70–80% RH, and a 16:8 h (L:D) photoperiod. The larvae and adults were reared with an artificial

98 diet and a 10% sugar solution, respectively. Pupae and newly laid eggs were sterilized with a 0.2–

99 0.3% sodium hypochlorite disinfectant solution (Wang et al., 2018b).

100 **2.2 | Insecticide and reagents**

101 Chlorantraniliprole (95%) was obtained from DuPont Agricultural Chemicals Co., Ltd. (Delaware,

102 USA). Triton X-100 was obtained from Amresco Co. (Texas, USA). All other chemicals, solvents,

103 and analytical grade reagents were obtained from Chengdu Aikeda Chemical Reagent Co., Ltd.

104 (Chengdu, China).

105 **2.3 | Reproductive system observation**

106 The newly hatched larvae were raised to pupae in glass tubes (diameter × height: 2.0 cm × 8.0 cm)

107 containing an artificial diet. The pupae were soaked in a 0.5% sodium hypochlorite solution and

108 disinfected. Three pairs of male and female of the SE-Sus strain or SE-Sel strains were placed in a

109 transparent plastic cup with a lid respectively. Each treatment was repeated eight times, and 10%

110 honey water was provided to nourish their eggs. The plastic cups and honey water were replaced

111 every 24 h, the eggs were collected, and the number of ovipositions per head (designated a) were

112 recorded until the end of oviposition. During the peak period of oviposition, 10 eggs were randomly

113 selected. After hatching, the number of hatched larvae (designated k) and the number of unhatched

114 larvae (designated m) were counted. After the female adult died, the ovaries were dissected under

115 an anatomical microscope to record the number of eggs left in the ovarian duct (considered

116 nonoviposition, b). The potential oviposition (designated n), oviposition rate, and hatchability were

117 calculated by the following formulas: potential oviposition $= a + b$; oviposition rate $= [a/n] \times$

118 100 %; and hatchability $= [k / (k + m)] \times 100\%$.

119 **2.4 | Ovary solution plane**

120 Forty SE-Sus and SE-Sel strains at the pupal stage were collected and separated with finger tubes,

121 and the weight of each pupa was recorded with an electronic balance after 24 h of pupation. After

122 24 h of eclosion, the female adults were weighed (designated c) under CO_2 anesthesia, washed in

123 clear water and put into phosphate buffered saline. The abdominal epidermis of the adults was torn

124 with two tweezers to expose the reproductive organs. The fat body and epidermis were removed as

125 far as possible, the ovaries were gently pulled out, and the ovarian tubes were gently moved with an

126 anatomical needle to fully expand the tubes. The length of the ovarian tubes was measured, and the

127 absorbent paper was removed. The fresh weight of the ovary (designated d) was measured and

128 recorded. The ovariole index was calculated using the following formula: Ovariole index $=$

129 $(c / d) \times 100\%$.

130 **2.5 | Gene expression pattern of SeVg in the SE-Sus and SE-Sel strains**

131 The SE-Sus and SE-Sel strains were fed in the finger tubes. When the larvae reached the prepupal

132 stage, they were transferred to a culture plate with artificial feed cells. Ten female pupae, from the

133 1st to the 8th day of pupation, and female adults emerged for 0, 12, 24, 36, 48, 60 and 72 h were

134 collected. The ovaries and fat bodies were obtained from the dissected pupae and dissected female

135 adults, loaded into 2 mL centrifugal tubes, instantly quick-frozen in liquid nitrogen and stored at

136 -80 ℃. RNA extraction, reverse transcription, and qPCR of the *SeVg* gene were performed in

137   accordance with the procedure described below.

2.6 | Transcriptome analysis

2.6.1 | Library construction and sequencing, splicing and unigenes annotation

In accordance with the manufacturer's instruction for the TRIzol® Reagent (Invitrogen™, ThermoFisher Scientific, Waltham, USA), approximately 10 ovaries and fat bodies of virgin adults emerged for 36 h from the SE-Sus and SE-Sel strains were used for total RNA isolation. cDNA library construction and sequencing, splicing, and unigenes annotation, covering Nr annotation, KEGG annotation, COG/KOG functional annotation and Gene Ontology (GO) annotation, were orderly performed according to the method described by Wang et al. (2018b).

2.6.2 | Gene expression and differential gene enrichment

The expression level of unigenes was figured by the RPKM method, according to the formula below: RPKM (A) = (1000000*C)/(N*L/1000) (Mortazavi et al., 2008). The RPKM (A) value denotes the expression level of gene A; the C value denotes the number of reads that uniquely mapped to gene A; the N value denotes the total number of reads that uniquely mapped to all genes, and the L value denotes the number of nucleic acid bases in gene A.

The dramatically differentially expressed genes (DEGs) between the SE-Sus and SE-Sel strains were screened by edge R. The screening threshold value were FDR < 0.05 (*P*-value after calibration by FDR) and |log2FC| > 1, and GO and KEGG enrichment analysis were performed for the DEGs.

2.6.3 | Quantitative PCR (qRT-PCR)

Total RNA of the ovaries and fat bodies of virgin adults emerged for 36 h from the SE-Sus and SE-Sel strains was extracted and reverse transcribed performed according to the procedure 2.6.1.

The cDNAs of Vg (*KT599434.1*), two ABC transporters (*SeABCG23* and *SeABCOK*), two transcription factors (*SETF* and *SESp9*), three glutathione *S*-transferase epsilons (*SeGST15, SeGST1* and *SeGSTZ2*), a carboxylesterase (*SeCarEs1*), two cytochrome P450s (*CYP6AEW* and *SeCYP6AB10*), two juvenile hormone-binding proteins (*SeJHBWDS3* and *SeJHBAN*), a vitellogenin receptor (*SeVgR*), a juvenile hormone diol kinase (*SeJHDK*), a sex peptide receptor (*SeSPR*), two

164   lebocin genes (*SeLE* and *SeLE2*), two cecropin genes (*SeCE* and *SeCEB*), a neuropeptide (*SeNPF*),

165   a neuropeptide receptor (*SeNPFR*) and the *F-actin* gene (Wang et al., 2016) from the SE-Sus and

166   SE-Sel strains were amplified by PCR with twelve pairs of corresponding primers (Table 1). The

167   system and procedure of qRT-PCR were performed according to the method described by Wang et

168   al. (2016).

169   **2.7 | Diversity and collinearity of neuropeptide genes**

170   A total of 63 complete neuropeptide amino acid sequences of *Drosophila melanogaster* and

171   *Spodoptera* insects were down loaded from NCBI database and analyzed for the conserved

172   functional domains with the motif search (https://www. genome.jp/ tools/ motif/) and meme (http:

173   //meme-suite. org/ tools/ meme) tools. The results were visualized with TBtools software.

174   **2.8 | Statistics and annotation of single erroneously paired nucleotides and sequence analysis**

175   **of RyR genes**

176   Based on the alignment results between the reads of the two treatments and the assembled unigenes

177   database used by TopHat2, single erroneously paired nucleotides (SNPs), as determined by

178   comparison with the assembled unigenes, were distinguished by The Genome Analysis Toolkit

179   (GATK) (McKenna et al., 2010), then these SNP sites were analyzed by the program SnpEff

180   (Cingolani et al., 2012). Furthermore, it was possible to analyze whether these SNP sites affected

181   the gene expression level or encoded protein type. On the basis of the cDNA fragments

182   (*Unigene0007287* and *Unigene0010376*) of RyR from RNA-seq data compared with ALL55470.1

183   in NCBI, we cloned the sequence containing the specific amino acids 4631-4967 of RyR. The

184   cDNAs of RyR genes were amplified by PCR with corresponding primer pairs (Table 2).

185   TransStart® FastPfu DNA Polymerase (TransGen Biotech, Beijing, China) was used in the PCR.

186   PCR was conducted with a PCR cycle of 95 ℃ for 2 min, 35 cycles of 95 ℃ for 20 s, 60 ℃ for 20 s

187   and 72 ℃ for 1 min, ending with an extension at 72 ℃ for 5 min. Amplified fragments were purified

188   by a TIANgel® Midi Purification Kit (Tiangen, Beijing, China) and sequenced at Shanghai

189   Biological Engineering Co., Ltd.

190   **2.9 | Data analysis**

191 The relative normalized expression of the screened genes and validated genes, the number of

192 oviposition, nonoviposition, hatched and unhatched larvae; the weights of pupae, female adults and

193 organs; and the length and number of the ovarian tubes in the SE-Sus and SE-Sel strains were

194 compared by using analysis of variance (ANOVA) followed by Duncan's test for multiple

195 comparisons ($P < 0.05$) with the SPSS version 17.0 software package (IBM).

3 | RESULTS

3.1 | Comparison of the reproductive capacity and egg hatchability between the SE-Sus and SE-Sel strains

199 The average number of ovipositions per female of the SE-Sus strain was 715.50, which was

200 significantly higher than that of the SE-Sel strain (181.79) (Figure 1A). After dissecting dead

201 female adults, the average number of nonoviposition per female for the SE-Sus strain only reached

202 66.17, and was significantly lower than that in the SE-Sel strain (457.29) (Figure 1A). Therefore,

203 the potential fecundity and oviposition rates of the SE-Sus strain were 781.67 and 91.08%,

204 respectively, which were significantly higher than those of the SE-Sel strain at 639.08 and 27.11%

205 (Figure 1A, Figure 1B). The gap in egg hatchability between SE-Sus and SE-Sel was only 2.16%,

206 with no significant difference (Figure 1B).

207

3.2 | Comparison of the ovariole index between the SE-Sus and SE-Sel strains

209 The mean pupal weights of each female and male of the SE-Sus strain were 0.0949 g and 0.089 g,

210 respectively, which were significantly lower than those of the SE-Sel strain (0.1086 g and 0.0974 g,

211 respectively) (Figure 2A).The mean weight of each female adult of the SE-Sus strain (0.0656 g)

212 was significantly less than that of the SE-Sel strain (0.0734 g), meanwhile the weight of preovary

213 and the length of ovarian tubes obtained from dissecting female adults of the SE-Sus strain (0.0286

214 g and 3.46 cm) were also lower than those of the SE-Sel strain (0.0300 g and 3.55 cm) even though

215 there was no difference ($P > 0.05$) (Figure 2A, Figure 2B); the ovariole index of female adults of

216 the SE-Sus strain (0.4382) was higher than that of the SE-Sel strain (0.4102), but the difference was

217 not significant (Figure 2B).

218   **3.3 | Gene expression pattern of SeVg in the SE-Sus and SE-Sel strains**

219   The relative expression of *SeVg* gene in SE-Sus and SE-Sel females was detected at different times
220   and the results indicated that the *SeVg* gene in the two strains began to express at the fifth day of
221   pupal stage. With the elongation and emergence of pupae, the expression level of *SeVg* gene firstly
222   increased until 36 h after emergence, reached the highest value, then began to decline. At 60 h after
223   emergence, the expression level reached the second highest value, and then decreased again. The
224   expression of *SeVg gene* in the SE-Sus strain was significantly stronger than that in the SE-Sel
225   strain ($P < 0.05$), except for the 6th, 8th days of pupation and 0 h, 48 after emergence (Figure 3).

226   **3.4 | Illumina sequencing and read assembly**

227   The total number of reads (150 bp / read) obtained from the SE-Sus and SE-Sel strains assessed in
228   triplicate was 296,690,624, with 42,072,370 reads at least for each sample. The proportion of reads
229   including linker sequences achieved 0.42 ~ 0.47%, and that of low-quality reads which included
230   reads with > 10% Ns and an abased number of $Q \leq 10$ in > 50% of the total reads reached
231   1.45~1.54%. After the linker sequences or low-quality reads filtered out, 290,810,118 clean reads
232   were received, and the Q20 and Q30 were more than 98.91% and 96.64%, respectively
233   (Supplementary Table 1).

234   **3.5 | Transcriptome data splicing**

235   The clean reads were constituted mixed pools and spliced into approximately 39,957 unigenes, and
236   the longest unigene contained 20,539 nt, but the shortest unigene contained 201 nt (Supplementary
237   Fig. 1A). The N50 value, that is, the cumulative fragmentary length reaches 50% of the total
238   fragmentary length, was 2,161 nt. There were 11,513 unigenes between 200-299 nt in length and
239   3,268 unigenes of over 3,000 nt in length. 4,295 unigenes contained over 10,000 reads, while
240   17,179 unigenes were composed of only 11~100 reads (Supplementary Figure **1**B).

241   **3.6 | Transcriptome annotation**

242   In the Nr database, 18,474 unigenes were successfully obtained exegeses, and the species (top 4)
243   with the greatest number of homologous genes were *Amyelois transitella* (3493), *Bombyx mori*
244   (3234), *Papilio xuthus* (1850), and *Papilio machaon* (1426), respectively (Supplementary Fig. 2A).

245 Additionally, 11,891 unigenes were annotated in the SwissProt database, 11,671 unigenes were

246 annotated in the KOG database, 11,891 unigenes were annotated in the KEGG database, and 8,020

247 unigenes were annotated in these four databases (Supplementary Figure 2B). Among the 11,671

248 unigenes annotated in the KOG database, 5,024 unigenes were categorized as general function

249 prediction only, accounting for the largest proportion, and 3,388 unigenes were categorized as

250 signal transduction mechanisms (Supplementary Figure 2C).

251 **3.7 | Analysis of gene expression**

252 The correlations of gene expression levels in the SE-Sus strains (with a correlation index of 0.9989

253 to 1.0000) were dramatically higher than those in the SE-Sel strains (with a correlation index of

254 0.9871 to 0.9906) (Figure 4A). Additionally, there was a significant clustering relationship on PC1

255 between the samples in the SE-Sus strain and the SE-Sel strain, respectively, and the contribution

256 degree of PC1 (96.8%) was dramatically higher than that of PC2 (2.1%) (Figure 4B).

257 **3.8 | Cluster analysis of DEGs**

258 Under the screening threshold value of FDR<0.05 and |log2FC|>1, 8,253 DEGs were obtained from

259 the SE-Sel strain in comparison with the SE-Sus strain, 4,020 of which were upregulated, while

260 4,233 were downregulated (Figure 5A and Figure 5B).

261 **3.9 | GO enrichment**

262 The DEGs were enriched and assessed in the three Gene Ontology (GO) categories of biological

263 process, cellular component, and molecular function. Among these DEGs enriched in molecular

264 function, catalytic activity (GO: 0003824) was the most abundant (109), accounting for 72.19%,

265 while in the cellular component category, cell (GO: 0005623) and cell part (GO: 0044464) were the

266 most abundant (34.4%), and in the biological process category, metabolic process (GO: 0008152)

267 was the most abundant (94), accounting for 65.73% (Supplementary Figure 3).

268 **3.10 | Enrichment of DEGs in the KEGG database**

269 A total of 385 DEGs were enriched in the KEGG database and were related to metabolism,

270 environmental information processing, and cellular processes. The enriched DEGs found in the

271 KEGG database were mainly in categories such as "biosynthesis of secondary metabolites" (with a

272 *P*-value of 4.72E-06), "neuroactive ligand-receptor interaction" (*P*-value of 1.82E-05), "metabolic

273 pathways" (*P*-value of 3.94E-05), "lysosome" (*p*-value of 0.000223), "glycine, serine and threonine

274 metabolism" (*p*-value of 0.000385), and "drug metabolism – other enzymes" *(p*-value of 0.00055).

275 Additionally, the greatest number of unigenes enriched in metabolic pathways was 163 (Figure 6).

276 **3.11 | Screening the candidate genes**

277 The results showed that among 39,957 unigenes, 487 unigenes were involved in the detoxification

278 and metabolism of foreign substances, including 85 cytochrome P450s, 329 cytochrome

279 transporters, 45 glutathione *S*-transferases, and 28 carboxylesterases, enriching the detoxification

280 and metabolism genes of *S. exigua*. Compared with the SE-Sus strain, the SE-Sel strain exhibited

281 22 significantly up- or downregulated DEG unigenes, annotated as ABC transporters, transcription

282 factors, glutathione *S*-transferases, carboxylesterases, cytochrome P450s, juvenile hormone-binding

283 proteins, vitellogenin receptors, juvenile hormone diol kinases, sex peptide receptors, lebocin,

284 cecropin, neuropeptides, and neuropeptide receptors (Supplementary Table 2).

285 **3.12 | Quantitative PCR (qRT-PCR)**

286 The results indicated that the relative normalized expression levels of the ABC transporter

287 *(SeABCOK)*, glutathione *S-transferases (SeGST15* and *SeGSTZ2)*, carboxylesterases *(SeCarEs1)*,

288 and cytochrome P450s *(CYP6AEW* and *SeCYP6AB10)* in the SE-Sel strain reached 3.27-, 3.81-,

289 3.64-, 2.25-, 2.70- and 2.98-fold, respectively and were significantly higher than those in the

290 SE-Sus strain (*P*< 0.05). In contrast, the relative normalized expression levels of the juvenile

291 hormone-binding protein *SeJHBWDS3,* vitellogenin receptor *SeVgR* and juvenile hormone diol

292 kinase *SeJHDK* in the SE-Sel strain were significantly decreased by 0.01-, 0.36-, and 0.31-fold (*P* <

293 0.05), whereas the sex peptide receptor *SeSPR,* neuropeptide *SeNPF,* and neuropeptide receptor

294 *SeNPFR* showed 3.04-, 4.33-and 16.39-fold increases, respectively, in the SE-Sel strain compared

295 with the SE-Sus strain (*P* < 0.05), and the relative normalized expression levels of the lebocin *SeLE*

296 and *SeLE2* genes and cecropin *SeCE* and *SeCEB* genes were significantly decreased by 0.84-, 0.78-,

297 0.26-, and 0.43-fold (*P* < 0.05) (Figure 7).

298 **3.13 | Neuropeptide diversity analysis**

Ten motifs (motif1~motif10), composed of highly conserved amino acid residues, were found in 63 *neuropeptide* amino acid sequences of *Drosophila melanogaster* and *Spodoptera* insects by meme search (http: //meme-suite.org/tools/ meme). In contrast, 41 motifs annotated with different functions were identified by motif search (https://www. genome.jp/ tools/ motif/) (e.g., Porin_5). All *neuropeptide* genes exhibited the conserved structural domains of motif5 but multifarious functional domains. Based on the structural domains and functional domains, the *neuropeptide* genes were divided into different subfamilies, such as PBAN, FMRF, allatostatin, neuropeptide Y and neuropeptide F. The PBAN (pheromone biosynthesis activating neuropeptide) family contains PBAN functional domains and a highly conserved domain (consisting of motif5, motif1 motif4, motif3, motif8, and motif2). The FMRF amide-related peptide family includes FARP functional domains and highly conserved residues (consisting of Phe-Met-Arg-Phe-NH$_2$). The allatostatin family has allatostatin functional domains and highly conserved residues (consisting of Tyr/Phe-Xaa-Phe-Gly-Leu/Ile-NH2), and it could inhibit juvenile hormone biosynthesis by the corpora allata. Neuropeptide Y possesses PAH functional domains and a highly conserved domain (consisting of motif5, motif1, and motif6). Neuropeptide F harbors N_NLPC_P60 and kinocilin functional domains and a highly conserved domain (consisting of motif5, motif1, motif6, and motif7). Not only highly homologous sequences but also functional domains, such as PAH (pancreatic hormone domain, neuropeptide Y), were found in *AXY04281.1* (the sequences of neuropeptide F2 in *S. exigua* downloaded from NCBI) and *SeNPF*. Therefore, these sequences were similar in function, and GO annotation showed that both were classified as neuropeptides and that *SeNPF* was classified as neuropeptide Y (Figure 8 and Supplementary Figure 4).

3.14 | Statistics and annotation of SNPs and sequence analysis of the RyR genes

Principal component analysis (PCA) and cluster dendrogram of the SNPs of six samples also showed that there was a significant clustering relationship in the samples of the SE-Sus strains (SE-Sus-1, SE-Sus-2, SE-Sus-3) and the SE-Sel strains (SE-Sel-1, SE-Sel-2, SE-Sel-3) (Supplementary Figure 5A and Supplementary Figure 5B). Additionally, the degree of the contribution of PC1 (60.3%) was significantly higher than that of PC2 (11.6%) (Supplementary Figure 5A). Some SNPs in *Unigene0007287* and *Unigene0010376* mapped to the specific amino acids 4631-4967 of RyR were identified through transcriptome data and sequence alignment

328 between the SE-Sus and the SE-Sel strains. The sequence mapped to the specific amino acids

329 4631-4967 of RyR showed that I4765M (ATA-ATG) in RyR was found in the SE-Sel strain

330 compared with the SE-Sus strain and ALL55470.1 in NCBI (Figure. 9).

331 **4 | DISCUSSION**

332 At present, the resistance of *S. exigua* to chlorantraniliprole is becoming increasingly serious.

333 Fortunately, the development of insecticide resistance is commonly accompanied by fitness costs,

334 along with the evolution of resistance (Ma et al., 2019). Ribeiro et al. (2013) revealed that the *P.*

335 *xylostella* of chlorantraniliprole-resistant field population presented a significantly lower larval

336 weight and fecundity than the susceptible strain when not exposed, suggesting a fitness cost

337 associated with resistance. When the resistant strain of *Nilaparvata lugens* was obtained by

338 continuous selection in the presence of nitenpyram, the resistant strain showed a lower intrinsic rate

339 of increase in the net reproductive rate, egg survival rate, and fecundity (eggs/female) compared to

340 the susceptible strain (Zhang et al., 2018). However, both of the resistant strains ImiLabSel and

341 ImiRes exhibited higher activities of cytochrome P450 monooxygenases by 72.3% and 40.5% and

342 severe fitness costs (reductions of 86% for ImiLabSel and 68.0% for ImiRes) (Castellanos et al.,

343 2019). Our data also indicated that the ability of potential oviposition and oviposition rate for per

344 female of the SE-Sel strain were significantly decreased when successively exposed to

345 chlorantraniliprole.

346   The formation and deposition of *Vg* is a fundamental step during the procedure of the

347 vitellogenesis of insects, which is a prerequisite for the regulation of insect reproduction and the

348 maturity of egg cell development (Amdam et al., 2010), and is traditionally considered a key factor

349 in the female fertility of insects (Zhao et al., 2018). The decreased expression of *Vg* exerted

350 negative impacts on the fecundity of *Chilo suppressalis* and *A. lucorum*, and there were

351 significantly positive linear correlations between *SeVg* and *SeVgR* expression in *S. exigua* (Huang et

352 al., 2016; Zhen et al., 2018; Zhao et al., 2018). Our results demonstrated that the mRNA expression

353 levels of *SeVg* and *SeVgR* were significantly reduced in the SE-Sel strain compared with the SE-Sus

354 strain and were consistent with the number of potential ovipositions. Shu et al. (2011) and Zhao et

355 al. (2016) also revealed that *Vg* was expressed specifically in the female fat body and was

356   detectable after the 5th day of female pupation, then reached a maximum in 48-h-old or 36-h-old

357   female adults and started to decrease quickly, which was similar to our results.

358   The *Vg* contents in the ovary depend not only on uptake by *VgR* into oocytes during

359   vitellogenesis but also on its synthesis affected by various elements, such as ecdysone and juvenile

360   hormone (JH) (Hansen et al,. 2015; Subala et al., 2017). Parthasarathy et al. (2010) confirmed that

361   JH directly regulated the synthesis of Vg in the fat body, and hibernation-triggered JH changes

362   resulted in the upregulation of *Vg1* and *Vg2* and the production of queens (Romain et al., 2013).

363   There is a significant relationship among JH titers and the biosynthesis of insect JHs is regulated by

364   juvenile hormone-binding proteins (transported to the target cells), juvenile hormone diol kinases

365   (catalyzes the formation of JHDP from JH diol) (Hidayat et al., 1994; Maxwell et al., 2002) and

366   neuropeptides, such as allatostatins (Stay and Tobe, 2007) and allatotropins (Elekonich and

367   Horodyski 2003). Neuropeptides also regulate the synthesis of Vg, and injections of corazonin

368   peptide caused a decrease in *Vg* mRNA levels (Gospocic et al., 2017). Our transcriptome data and

369   qRT-PCR results also indicated that the expression levels of *Se*NPF and *Se*NPFR were significantly

370   increased, even though those of the juvenile hormone-binding protein and juvenile hormone diol

371   kinase significantly decreased in the SE-Sel strain compared with the SE-Sus strain; this could

372   explain why the expression levels of *Se*Vg and *SeVgR* in the SE-Sel strain were low.

373   Except for the difference in potential oviposition, the oviposition rate was also significantly

374   lower because most of the eggs of SE-Sel strain remained in the ovaries. Oviposition was stimulated

375   after copulation, known as the postmating responses (PMRs) in inseminated females, which was

376   mediated by the (sex-peptide) SP/SPR (sex-peptide receptor) system (Oh et al., 2014; Tsuda et al.,

377   2016). PMRs require SPR in a limited number of sensory neurons in the female reproductive organ,

378   and the knockdown of *SPR* in either fruitless or pickpocket expressing neurons fails to induce PMR

379   after mating (Hasemeyer et al., 2009). However, the expression levels of SeSPR, *Se*NPF, and

380   *Se*NPFR in virgin adults of the SE-Sus strain were significantly increased compared with the

381   SE-Sus strain. Then, neuropeptide F expression levels and intracellular Ca^{2+} activity (as an indicator

382   of neural activation) in NPF neurons were altered by the animal's mating status (Yao et al., 2012;

383   Shohat-Ophir et al., 2012; Gao et al., 2015). Liu et al. (2019) found that knocking out *NPF*, a

384   homolog of the mammalian neuropeptide Y, or suppressing the activity of NPF neurons reduced the

385   inhibition of courtship behavior in sexually satiated males. Tuelher et al. (2017) also found that

386   chlorantraniliprole-treated males coupled with untreated females exhibited a higher number of

387   mating events because the release and depletion of Ca^{2+} might affect the activity of NPF neurons.

388   Phylogenetic tree analyses and gene molecular structure comparisons showed that there was high

389   homology between neuropeptide F2 *AXY04281.1* and neuropeptide *SeNPF*. All neuropeptide F and

390   neuropeptide Y family members in *Drosophila melanogaster* and *Spodoptera* insects had motif5,

391   motif6, and motif1, but other neuropeptide families did not have a similar structure. Therefore, we

392   speculate that the upregulation of neuropeptide *SeNPF* resulted in a lower probability of mating and

393   oviposition rate and may be the direct cause of the fitness cost of the SE-Sel strain. Gospocic et al.

394   (2017) found that the overexpression of neuropeptide and neuropeptide receptor stimulated insect

395   feeding and increased body weights of pupae and adults, similar to our results. The expression of

396   antimicrobial peptides, small cationic peptides with broad-spectrum antimicrobial activities that are

397   mainly synthesized by adipose somatic cells, such as lebocin and cecropin, could be induced by

398   mating (Lawniczak and Begun, 2004; McGraw et al., 2004), which is also similar to our results.

399   Our results of transcriptome analysis and cloning revealed the RyR^{I4765M} mutation in the

400   SE-Sel strain. Mutation in RyR (such as T4826I) could cause a gain-of-function, i.e., Ca^{2+} leakage

401   from the sarcoplasmic reticulum (Lyfenko et al., 2004; Robinson et al., 2006), which regulates

402   neuropeptide activation (James et al., 2014; McKinney et al., 2016; Truong et al., 2019).

403   Chlorantraniliprole engaged critical residues within the C-terminal transmembrane assembly, in

404   particular, the amino acids 4610-4946 and 4631-4967 in *S. exigua*, according to BLAST analysis

405   (Tao et al., 2013). The wicked evolution of these regions in targets made it less susceptible to the

406   action of the pesticide (Gould et al., 2018). Guo et al. (2014a and 2014b) discovered that there was

407   a significant correlation between the frequency of mutation (G4946E and I4790M) in RyR and the

408   chlorantraniliprole resistance ratios in *P. xylostella*. The RyR^{G4946E} mutation introduced with

409   CRISPR/Cas9 technology into the susceptible strain of *S. exigua* led to 223-fold resistance to

410   chlorantraniliprole (Zuo et al., 2017). In addition to target-mediated resistance, the overexpression

411   of detoxification metabolism genes, MFOs, carboxylesterases (CarEs), glutathione *S*-transferases

412   (GSTs) and ABC transporters, increases the efficiency of an enzyme that degrades the insecticide

413   (Chen et, al. 2012; Hu et al., 2014; Tian et al., 2014; Lu et al., 2017; Wang et al., 2018a; Xu et al.,

2019). Our transcriptome data and qRT-PCR results also indicated that ABC transporter *SeABCOK*, glutathione S-transferases *SeGST15* and *SeGSTZ2*, carboxylesterases *SeCarEs1*, and cytochrome P450s *CYP6AEW* and *SeCYP6AB10* were clearly upregulated in the SE-Sel strain. However, Silva et al. (2019) found that the wicked evolution of RyR led to the increase in the resistance to chlorantraniliprole in the tomato pinworm *Tuta absoluta* rather than enhanced detoxification. Thus, the evolution of RyR might have a greater impact on resistance evolution, but this requires further verification. Therefore, the increase of the resistance to chlorantraniliprole in the SE-Sel strain, accompanied by the fitness cost, was the result of the wicked evolution of RyR, but how RyR mutation affects the upregulation of neuropeptides and induces a fitness cost requires further verification.

5 | CONCLUSIONS

On the basis of our results, the main findings showed that *S. exigua* would likely further improve in resistance to chlorantraniliprole, owing to the upregulation of detoxification enzymes, such as ABC transporters, GSTs, CarEs and P450s, and the wicked evolution of RyR. However, we also showed that the fitness costs were accompanied by the development of insecticide resistance; for example, the potential oviposition and the oviposition rate of the SE-Sel strain were significantly lower than those of the SE-Sus strain because the expression of *SeVg* and *SeVgR* in the SE-Sel strain were always lower than those in the SE-Sus strain. Moreover, the RyR mutation could affect the activities of neuropeptides, it conduced to the upregulated expression of the neuropeptide *SeNPF* and its receptor, *SeNPFR*, which could inhibit courtship behavior and reduce oviposition. And the neuropeptide *SeNPF* could influence the expression of *juvenile hormone-binding protein* and *juvenile hormone diol kinase*, and it led to the downregulated expression of *SeVg*. Therefore, these results indicate that the fitness cost accompanied by chlorantraniliprole resistance in *S. exigua* is related to the wicked evolution of RyR. We also found that the relative normalized expression of lebocin and cecropin was significantly decreased; therefore, the combination of RyR activator insecticide and insect virus preparation might be more effective in controlling insect resistance.

REFERENCES

Abbas, N., Samiullah, Shad, S.A., Razaq, M., Waheed, A., & Aslam, M. (2014). Resistance of *Spodoptera litura* (Lepidoptera: Noctuidae) to profenofos: relative fitness and cross resistance. *Crop Protectionection*, 58, 49–54. https://doi.org/10.1016/j.cropro.2014.01.002

Abbas, N., Shah, R.M., Shad, S.A., & Azher, F. (2016). Dominant fitness costs of resistance to fipronil in *Musca domestica* Linnaeus (Diptera: Muscidae). *Veterinary Parasitology*, 226, 78–82. https://doi.org/10.1016/j.vetpar.2016.06.035

Amdam, G.V., Page, R.E., Fondrk, M.K., & Brent, C.S. (2010). Hormone response to bidirectional selection on social behavior. *Evolution & Development*, 12, 428–436. https://doi.org/10.1111/j.1525-142X.2010.00429.x

Cao, G.C., & Han, Z.J. (2006). Tebufenozide resistance selected in *Plutella xylostella* and its cross-resistance and fitness cost. *Pest Management Science*, 62, 746–751. https://doi.org/10.1002/ps.1234

Castellanos, N.L., Haddi, K., Carvalho, G.A., de Paulo, P.D., Hirose, E., Guedes, R.N.C., Smagghe, G., & Oliveira, E.E. (2019). Imidacloprid resistance in the Neotropical brown stink bug *Euschistus heros*: selection and fitness costs. *Journal of Pest Science*, 92, 847–860. https://doi.org/10.1007/s10340-018-1048-z

Che, W.N., Shi, T., Wu, Y.D., & Yang, Y.H. (2013). Insecticide resistance status of field populations of *Spodoptera exigua* (Lepidoptera: Noctuidae) from China. *Journal of Economic Entomology*, 106, 1855–1862. https://doi.org/10.1603/EC13128

Chen, E.H., Dou, W., Hu, F., Tang, S., & Wang, J.J. (2012). Purification and biochemical characterization of glutathione *S*-transferases in *Bactrocera minax* (Diptera: Tephritidae). *Florida Entomologist,* 95, 593–601. https://doi.org/10.1653/024.095.0309

Cingolani, P., Platts, A., Wang, L.L., Coon, M., Nguyen, T., Wang, L., Land, S.J., Lu, X.Y., & Ruden, D.M. (2012). A program for annotating and predicting the effects of single erroneously paired nucleotides, SnpEff: SNPs in the genome of *Drosophila melanogaster* strain w_{1118}; iso-2; iso-3. *Fly*, 6, 80–92. https://doi.org/10.4161/fly.19695

David, B.S., Daniel, C., & Timothy, R.C. (2008). Insect ryanodine receptors: molecular targets for novel pest control chemicals. *Invertebrate neuroscience*, 8, 107–119. https://doi.org/10.1007/s10158-008-0076-4

Elekonich, M.M., & Horodyski, F.M. (2003). Insect allatotropins belong to a family of structurally myoactive peptides present in several invertebrate phyla. *Peptides*, 24, 1623–1632. https://doi.org/10.1016/j.peptides.2003.08.011

Gao, C., Yao, R., Zhang, Z., Wu, M., Zhang, S., & Su, J. (2013). Susceptibility baseline and chlorantraniliprole resistance monitoring in *Chilo suppressalis* (Lepidoptera: Pyralidae). Journal of Economic Entomology, 106, 2190–2194. https://doi.org/10.1603/EC13058

Gao, X.J., Riabinina, O., Li, J., Potter, C.J., Clandinin, T.R., & Luo, L. (2015). A transcriptional reporter of intracellular Ca^{2+} in Drosophila. *Nature Neuroscience*, 18, 917–925.

Giorgi, F., Bradley, J.T., & Nordin, J.H. (1999). Differential vitellin polypeptide processing in insect embryos. *Micron*, 30, 579–596. https://doi.org/10.1016/S0968-4328(99)00054-2

Gospocic, J., Shields, E.J., Glastad, K.M., Lin, Y., Penick, C.A., Yan, H., Mikheyev, A.S., Linksvayer, T.A., Garcia, B.A., Berger, S.L., Liebig, J., Reinberg, D., Bonasio, R. (2017). The neuropeptide corazonin controls social behavior and caste identity in ants. *Cell*, 170, 748–759(e12). https://doi.org/10.1016/j.cell.2017.07.014

Gould, F., Brown, Z.S., & Kuzma, J. (2018). Wicked evolution: Can we address the sociobiological dilemma of pesticide resistance? *Science*, 360, 728–732. https://doi.org/10.1126/science.aar3780

Guo, L., Liang, P., Zhou, X., & Gao, X.W. (2014a). Novel mutations and mutation combinations of ryanodine receptor in a chlorantraniliprole resistant population of *Plutella xylostella* (L.). *Scientific Reports*, 4, 6924.

Guo, L., Wang, Y., Zhou, X.G., Li, Z.Y., Liu, S.Z., Pei, L., & Gao, X.W. (2014b) Functional analysis of a point mutation in the ryanodine receptor of *Plutella xylostella* (L.) associated with resistance to chlorantraniliprole.

486   *Pest Management Science,* 70, 1083–1089. https://doi.org/10.1002/ps.3651

487 Hansen, I.A., Attardo, G.M., Roy, S.G., & Raikhel, A.S. (2005). Target of rapamycin-dependent activation of S6
488   kinase is a central step in the transduction of nutritional signals during egg development in a mosquito. *The*
489   *Journal of biological chemistry*, 280 (20)565–20572. https://doi.org/10.1074/jbc.M500712200

490 Hasemeyer, M., Yapici, N., Heberlein, U., & Dickson, B.J. (2009). Sensory neurons in the *Drosophila* genital
491   tract regulate female behavior. *Neuron*, 61, 511–518. https://doi.org/10.1016/j.neuron.2009.01.009

492 Hidayat, P., & Goodman, W.G. (1994). Juvenile hormone and hemolymph juvenile hormone binding protein titers
493   and their interaction in the hemolymph of fourth stadium *Manduca sexta*. *Insect Biochemistry and Molecular*
494   *Biology*, 24, 709-715. https://doi.org/10.1016/0965-1748(94)90058-2

495 Hu, Z.D., Feng, X., Lin, Q.S., Chen, H.Y., Li, Z.Y., Yin, F., Liang, P., & Gao, X.W. (2014). Biochemical
496   mechanism of chlorantraniliprole resistance in the diamondback moth, *Plutella xylostella* Linnaeus. *Journal*
497   *of Integrative Agriculture*, 13, 2452–2459.

498 Huang, L., Lu, M.X., Han, G.J., Du, Y.Z., & Wang, J.J. (2016). Sublethal effects of chlorantraniliprole on
499   development, reproduction, and vitellogenin gene (CsVg) expression in the rice stem borer, *Chilo*
500   *suppressalis*. *Pest Management Science*, 72, 2280–2286. https://doi.org/10.1002/ps.4271

501 Huang, Q., Wang, X.G., Yao, X.G., Gong, C.W., & Shen, L.T. (2019). *Effects of bistrifluron resistance on the*
502   *biological traits of Spodoptera litura* (Fab.) (Noctuidae Lepidoptera). *Ecotoxicology*, 28, 323–332.
503   https://doi.org/10.1007/s10646-019-02024-2

504 James, M.M., Edward, E.C., Sonia, O.M., Dixon, J.W., Susan, D.K., Brian, M.S., et al. (2014). Functional
505   ryanodine receptors in the membranes of neurohypophysial secretory granules. *The Journal of general*
506   *physiology*, 143, 693–702. https://doi.org/10.1085/jgp.201311110

507 Kliot, A., & Ghanim, M. (2012). Fitness costs associated with insecticide resistance. *Pest Management Science*,
508   68:1431–1437. https://doi.org/10.1002/ps.3395

509 Lahm, G.P., Selby, T.P., Freudenberger, J.H., Stevenson, T.M., Myers, B.J., Seburyamo, G., Smith, B.K., Flexner,
510   L., Clark, C.E., Cordova, D. (2005). Insecticidal anthranilic diamides: a new class of potent ryanodine
511   receptor activators. *Bioorganic & medicinal chemistry letters*, 15, 4898–4906.
512   https://doi.org/10.1016/j.bmcl.2005.08.034

513 Lai, T.C., Li, J., & Su, J.Y. (2011). Monitoring of beet armyworm *Spodoptera exigua* (Lepidoptera: Noctuidae)
514   resistance to chlorantraniliprole in China. *Pesticide Biochemistry and Physiology*, 101, 198–205.
515   https://doi.org/10.1016/j.pestbp.2011.09.006

516 Lawniczak, M.K., & Begun, D.J. (2004). A genome–wide analysis of courting and mating responses in
517   *Drosophila melanogaster* females. *Genome*, 47, 900–910. https://doi.org/10.1139/g04-050

518 Liu, W., Ganguly, A., Huang, J., Wang, Y., Ni, J.D., Gurav, A.S., Aguilar , M.A., Montell, C. (2019).
519   Neuropeptide F regulates courtship in *Drosophila* through a male-specific neuronal circuit. *Elife*, 12:8.
520   https://doi.org/10.7554/eLife.49574

521 Lu, Y.H., Wang, G.R., Zhong, L.Q., Zhang, F.C., Bai, Q., Zheng, X.S., Lu, Z.X. (2017). Resistance monitoring of
522   *Chilo suppressalis* (Walker) (Lepidoptera: Crambidae) to chlorantraniliprole in eight field populations from
523   east and central China. *Crop Protection*, 196–202. https://doi.org/10.1016/j.cropro.2017.07.006

524 Lyfenko, A.D., Goonasekera, S.A., & Dirksen, R.T. (2004). Dynamic alterations in myoplasmic Ca^{2+} in malignant
525   hyperthermia and central core disease. *Biochemical and Biophysical Research Communications*, 322,
526   1256-1266. https://doi.org/10.1016/j.bbrc.2004.08.031

527 Ma, K.S., Tang, Q.L., Xia, J., Lv, N.N., & Gao, X.W. (2019). Fitness costs of sulfoxaflor resistance in the cotton
528   aphid, *Aphis gossypii* Glover. *Pesticide Biochemistry and Physiology*, 40–46.
529   https://doi.org/10.1016/j.pestbp.2019.04.009

530 Maxwell, R.A., Welch, W.H., Horodyski, F.M., Schegg, K.M., & Schooley, D.A. (2002). Juvenile hormone diol
531   kinase. II. Sequencing, cloning, and molecular modeling of juvenile hormone-selective diol kinase from
532   *Manduca sexta*. *The Journal of Biological Chemistry*, 21882–21890.

533   https://doi.org/10.1074/jbc.M201509200

534 McGraw, L.A., Gibson, G., Clark, A.G., *& Wolfner, M.F. (2004). Genes regulated by mating, sperm, or seminal
535   proteins in mated female *Drosophila melanogaster.Current Biology*, 14, 1509–1514.

536 McKenna, A., Hanna, M., Banks, E., Sivachenko, A., Cibulskis, K., Kernytsky, A. Garimella, K., Altshuler, D.,
537   Gabriel, S., Daly, M., DePristo, M.A. (2010). The genome analysis toolkit: a mapreduce framework for
538   analyzing next-generation DNA sequencing data. *Genome Research*, 20, 1297–1303.

539 McKinney, D.A., Eum, J.H., Dhara, A., Strand, M.R., *& Brown, M.R. (2016). Calcium influx enhances
540   neuropeptide activation of ecdysteroid hormone production by mosquito ovaries. Insect Biochem. *Insect
541   Biochemistry and Molecular Biology*, 160–169. https://doi.org/10.1016/j.ibmb.2016.01.001

542 Mortazavi, A., Williams, B.A., McCue, K., Schaeffer, L., *& Wold, B. (2008). Mapping and quantifying
543   mammalian transcriptomes by RNA-Seq. Nature Methods, 5, 621–628.

544 Moulton, J.K., Pepper, D.A., Jansson, R.K., *& Dennehy, T.J. (2002). Pro-active management of *beet armyworm*
545   (Lepidoptera: Noctuidae) resistance to tebufenozide and methoxyfenozide: baseline monitoring, risk
546   assessment, and isolation of resistance. *Journal of Economic Entomology*, 95, 414–424.
547   https://doi.org/10.1603/0022-0493-95.2.414

548 Oh, Y., Yoon, S.E., Zhang, Q., Chae, H,S., Daubnerova, I., Shafer, O.T., Choe, J., *& Kim, Y.J. (2014). A
549   homeostatic sleep-stabilizing pathway in Drosophila composed of the sex peptide receptor and its ligand, the
550   myoinhibitory peptide. *Plos Biology*, 12, e1001974. https://doi.org/10.1371/journal.pbio.1001974

551 Parthasarathy, R., Sun, Z.Y., Bai, H., *& Palli, S.R. (2010). Juvenile hormone regulation of vitellogenin synthesis
552   in the red flour beetle, *Tribolium castaneum. Insect Biochemistry and Molecular Biology*, 40, 405–414.
553   https://doi.org/10.1016/j.ibmb.2010.03.006

554 Passos, D.A., Silva-Torres, C.S.A., *& Siqueira, H.A.A. (2019). Behavioral response and adaptive cost in resistant
555   and susceptible *Plutella xylostella* to chlorantraniliprole. *Bulletin of Entomological Research*, 1–10.
556   https://doi.org/10.1017/S0007485319000300

557 Ribeiro, L.M.S., Wanderley-Teixeira, V., Ferreira, H.N., Teixeira, A.A.C., *& Siqueira, H.A.A. (2013). Fitness
558   costs associated with field-evolved resistance to chlorantraniliprole in *Plutella xylostella* (Lepidoptera:
559   Plutellidae). *Bulletin of Entomological Research*. 1–9. https://doi.org/10.1017/S0007485313000576

560 Robinson, R., Carpenter, D., Shaw, M.A., Halsall, J., *& Hopkins, P. (2006). Mutations in RYR1 in malignant
561   hyperthermia and central core disease. *Human mutation*, 27, 977–989.

562 Romain, L., Miguel, C., Franziska, W., Dihego, O.A., Jose, E.S., *& Laurent, K. (2013). Interplay between insulin
563   signaling, juvenile hormone, and vitellogenin regulates maternal effects on polyphenism in ants. *Proceedings
564   of the National Academy of Sciences of the United States of America*, 10, 11050–11055.

565 Shohat-Ophir, G., Kaun, K.R., Azanchi, R., Mohammed, H., *& Heberlein, U. (2012). Sexual deprivation increases
566   ethanol intake in *Drosophila. Science*, 335, 1351–1355. https://doi.org/10.1126/science.1215932

567 Shu, Y.H., Wang, J.W., Lu, K., Zhou, J.L., Zhou, Q., *& Zhang, G.R. (2011). The first vitellogenin receptor from a
568   Lepidopteran insect: molecular characterization, expression patterns and RNA interference analysis. *Insect
569   Molecular Biology*, 20, 61–73. https://doi.org/10.1111/j.1365-2583.2010.01054.x

570 Silva, J.E., Ribeiro, L.M.S., Vinasco, N., Guedes, R.N.C., *& Siqueira, H.A.A. (2019). Field-evolved resistance to
571   chlorantraniliprole in the tomato pinworm *Tuta absoluta*: inheritance, cross-resistance profile, and
572   metabolism. *Journal of Pest Science,* 92, 1421–1431. https://doi.org/10.1007/s10340-018-1064-z

573 Stay, B., *& Tobe, S.S. (2007). The role of allatostatins in juvenile hormone synthesis in insects and crustaceans.
574   *Annual Review of Entomology*, 52, 277–299. https://doi.org/10.1146/annurev.ento.51.110104.151050

575 Su, J.Y., *& Sun, X.X. (2014.) High level of metaflumizone resistance and multiple insecticide resistance in field
576   populations of *Spodoptera exigua* (Lepidoptera: Noctuidae) in Guangdong Province, China. *Crop Protection*.
577   61, 58–63. https://doi.org/10.1016/j.cropro.2014.03.013

578 Subala, P.R., & Shivakumar, M.S. (2017). Circadian variation affects the biology and digestive profiles of a
579   nocturnal insect *Spodoptera litura* (Insecta: Lepidoptera). *Biological Rhythm Research*, 48, 207–226.
580   https://doi.org/10.1080/09291016.2016.1251928

581 Sun, L., Qiu, G.S., Li, C., Ma, C.S., & Yuan, H.Z. (2015). Molecular characterization of a ryanodine receptor
582   gene from *Spodoptera exigua* and its upregulation by chlorantraniliprole. *Pesticide Biochemistry and*
583   *Physiology*, 123, 56–63. https://doi.org/10.1016/j.pestbp.2015.03.002

584 Tao, Y., Gutteridge, S., Benner, E.A., Wu, L., Rhoades, D.F., Sacher, M.D., Desaeger, J., Cordova, D. (2013).
585   Identification of a critical region in the Drosophila ryanodine receptor that confers sensitivity to diamide
586   insecticides. *Insect Biochemistry and Molecular Biology*, 43, 820–828.
587   https://doi.org/10.1016/j.ibmb.2013.06.006

588 Teixeira, L.A., & Andaloro, J.T. (2013). Diamide insecticides: global efforts to address insect resistance
589   stewardship challenges. *Pesticide Biochemistry and Physiology*, 106, 76–78.
590   https://doi.org/10.1016/j.pestbp.2013.01.010

591 Tian, X.R., Sun, X.X., & Su, J.Y. (2014). Biochemical mechanisms for metaflumizone resistance in beet
592   armyworm, *Spodoptera exigua*. *Pesticide Biochemistry and Physiology*, 113, 8–14.
593   https://doi.org/10.1016/j.pestbp.2014.06.010

594 Truong, K.M., & Pessah, I.N. (2019). Comparison of chlorantraniliprole and flubendiamide activity toward
595   wild-type and malignant hyperthermia-susceptible ryanodine receptors and heat stress intolerance.
596   *Toxicological Sciences*, 167, 509–523. /

597 Tsuda, M., & Aigaki, T. (2016). Evolution of sex-peptide in *Drosophila*. *Fly,* 10, 172-177. /

598 Tuelher, E., da Silva, É.H., Freitas, H., Namorato, F., Serrão, J., Guedes, R., Oliveira, E. (2017).
599   Chlorantraniliprole- mediated toxicity and changes in sexual fitness of the Neotropical brown stink bug
600   *Euschistus heros*. *Journal of Pest Science*, 90, 397–405.

601 Tufail, M., Nagaba, Y., Elgendy, A.M., & Takeda, M. (2014). Regulation of vitellogenin genes in insects.
602   Entomological Science, 17, 269–282. https://doi.org/10.1111/ens.12086

603 Wahli, W., (1988). Evolution and expression of vitellogenin genes. *Trends in Genetics*, 4, 227-232.
604   https://doi.org/10.1016/0168-9525(88)90155-2

605 Wang, X., & Wu, Y. (2012). High levels of resistance to chlorantraniliprole evolved in field populations of
606   *Plutella xylostella*. *Journal of Economic Entomology*, 105, 1019–1023. https://doi.org/10.1603/EC12059

607 Wang, X.G., Chen, Y.Q., Gong, C.W., Yao, X.G., Jiang, C.X., & Yang, Q.F. (2018a). Molecular identification of
608   four novel cytochrome P450 genes related to the development of resistance of *Spodoptera exigua*
609   (Lepidoptera: Noctuidae) to chlorantraniliprole. *Pest Management Science*, 74, 1938–1952.
610   https://doi.org/10.1002/ps.4898

611 Wang, X.G., Gao, X.W., Liang, P., Shi, X.Y., & Song, D.L. (2016.) Induction of cytochrome P450 activity by the
612   interaction of chlorantraniliprole and sinigrin in the *Spodoptera exigua* (Lepidoptera: Noctuidae).
613   *Environmental Entomology*, 45, 500–507. https://doi.org/10.1093/ee/nvw007

614 Wang, X.G., Xiang, X., Yu, H.L., Liu, S.H., Yin, Y., Cui, P. et al. (2018b). Monitoring and biochemical
615   characterization of beta-cypermethrin resistance in *Spodoptera exigua* (Lepidoptera: Noctuidae) in Sichuan
616   Province, China. *Pesticide Biochemistry and Physiology*, 71–79.
617   https://doi.org/10.1016/j.pestbp.2018.02.008

618 Wu, G., Guo, J.Y., Wan, F.H., & Xiao, N.W. (2010). Responses of three successive generations of beet
619   armyworm, *Spodoptera exigua*, fed exclusively on different levels of gossypol in cotton leaves. *Journal of*
620   *Insect Science*, 10, 764–800. https://doi.org/10.1673/031.010.14125

621 Xu, L., Zhao, J., Sun, Y., Xu, D.J., Xu, G.C., Xu, X.L., Han, Z.J., & Gu, Z.Y. (2019). Constitutive overexpression
622   of cytochrome P450 monooxygenase genes contributes to chlorantraniliprole resistance in *Chilo suppressalis*

623   (Walker). *Pest Management Science*, 75, 718–725. https://doi.org/10.1002/ps.5171

624 Yao, Z., Macara, A.M., Lelito, K.R., Minosyan, T.Y., & Shafer, O.T. (2012). Analysis of functional neuronal

625   connectivity in the Drosophila brain. *Journal of Neurophysiology*, 108, 684–696.

626   https://doi.org/10.1152/jn.00110.2012

627 Zhang, P., Gao, M., Mu, W., Zhou, C., & Li, X.H. (2014). Resistant levels of *Spodoptera exigua* to eight various

628   insecticides in Shandong, China. *Journal of Pesticide Science*, 39, 7–13.

629   https://doi.org/10.1584/jpestics.D13-053

630 Zhang, X.L., Mao, K.K., Liao, X., He, B.Y., Jin, R.H., Tang, T., Wan, H., Li, J.H. (2018.) Fitness cost of

631   nitenpyram resistance in the brown planthopper *Nilaparvata lugens*. *Journal of Pest Science*, 91, 1145–1151.

632   https://doi.org/10.1007/s10340-018-0972-2

633 Zhao, J., Sun, Y., Xiao, L., Tan, Y., Jiang, Y., & Bai, L. X. (2018). Vitellogenin and vitellogenin receptor gene

634   expression profiles in *Spodoptera exigua* are related to host plant suitability. *Pest Management Science*, 74,

635   950–958. https://doi.org/10.1002/ps.4794

636 Zhao, J., Sun, Y., Xiao, L.B., Tan, Y.A., & Bai, L.X. (2016). Molecular characterization and expression of

637   Vitellogenin gene from *Spodoptera exigua* exposed to cadmium stress. *Gene*, 593, 179–184.

638   https://doi.org/10.1016/j.gene.2016.08.025

639 Zhen, C.A., Miao, L., & Gao, X.W. (2018). Sublethal effects of sulfoxaflor on biological characteristics and

640   vitellogenin gene (AlVg) expression in the mirid bug, *Apolygus lucorum* (Meyer-Dür). *Pesticide*

641   *Biochemistry and Physiology*, 144, 57–63. https://doi.org/10.1016/j.pestbp.2017.11.008

642 Zheng, X.L., Pan, W., Cheng, W.J., Wang, X.P., & Lei, C.L. (2012). Projecting overwintering regions of the beet

643   armyworm, *Spodoptera exigua*, in China using the CLIMEX Model. *Journal of Insect Science*, 12, 1–13.

644   https://doi.org/10.1673/031.012.1301

645 Zhou, C., Liu, Y.Q., Yu, W.L., Deng, Z.R., Gao, M., Liu, F., Mu, W. (2011). Resistance of *Spodoptera exigua* to

646   ten insecticides in Shandong, China. *Phytoparasitica*, 39, 315–324. https://doi.org/10.1007/

647   s12600-011-0157-5

648 Zuo, Y.Y., Wang, H., Xu, Y.J., Huang, J.L., Wu, S.W., Wu, Y.D., Yang, Y.H. (2017). CRISPR/Cas9 mediated

649   *G4946E* substitution in the ryanodine receptor of *Spodoptera exigua* confers high levels of resistance to

650   diamide insecticides. *Insect Biochemistry and Molecular Biology*, 89, 79–85.

651   https://doi.org/10.1016/j.ibmb.2017.09.005

SUPPORTING INFORMATION

657 Additional supporting information may be found online in the Supporting Information section.

658

659   **TABLE 1** Primers of differentially expressed gene for qRT-PCR

Gene	Prime	Squence (5'-3')	Length
SeSPR	4099-F	AGAGCGTGTCAAGCATGGAA	142
	4099-R	TTGTACACCATGTCCGAGCG	
CYP6AEW	4495-F	AAAAAGAATGTACCGCACGCC	148
	4495-R	CCGTTCCGTAGTAAGCTCCA	
SeLE2	5787-F	CATCCTGGATATAATCGACGCA	113

	5787-R	CTAGCTGCTCCCAATTGCTC	
SeABCG23	6176-F	TGGAAGCTACGGAGCACTTG	124
	6176-R	GGTCCAGCGAAGTCAGTCAA	
SeTF	8289-F	TGTGATGTTGAGGATGTACCGA	137
	8289-R	TCGTCAAAATCAGATGGCAAGC	
SeSp9	9845-F	GCTGAAATGAGCGGCGTTAG	199
	9845-R	GTGTTGGCAGCACAGACTTG	
SeCEB	11921-F	CTCCCGAGCCACGATGGAAA	105
	11921-R	CTGATCCCACAACGGCCACT	
SeVgR	12209-F	CCCAGGAAGAGAATGTTAGCGA	116
	12209-R	GGTAGATACCTTGAGGGGTGC	
SeABCOK	15443-F	GCTGGTAGTATGCTCGGTCC	106
	15443-R	TTCAATGGTCCCGTGGAAGG	
SeJHBWDS3	16076-F	CTAGTAACGCAAGCCACGGT	145
	16076-R	GAACTTCGGTGCCAACCTCT	
SeJHDK	18681-F	ACACTGGCACATCGACAACT	146
	18681-R	CACGCATAACATCACGCCAG	
SeJHBAN	18636-F	CAAGAACCCATCCGAAGCCT	149
	18636-R	CCACAGCCTCGTCTTTGTCT	
SeGST15	19590-F	CCCGGAGGTGTAGCCAAAAT	169
	19590-R	TGTTGGGGTACGTTGCTTCA	
SeLE	19665-F	GACATCAAGCTGGACCCCAA	126
	19665-R	GTTGTACCCCGGATGAGTGG	
SeGST1	20364-F	CCGTGCCATCAGCAGATACT	182
	20364-R	CATCGTCAGCTTTTGCTCCG	
SeGSTZ2	21647-F	AGGGAACTCTGTGAGGTGGT	124
	21647-R	TTAAGCCACGGTCAGTCCAG	
SeCarEs1	27390-F	TCGATGTGCTCGGCTTTCTT	120
	27390-R	GGTCACCACCGAAGTTAGCA	

SeCE	28139-F	TTCTCTCGTGTGTTTTTGTTTGTT	84
	28139-R	GACCTTCCATCTTGGTTCTGGC	
SeCYP6AB10	34483-F	TTCATCGGTGTCTGCGCATT	131
	34483-R	ATAATCTTCAGGGCACCGGC	
SeNPFR	35241-F	TAGGCGAGGCTTCAAACAGG	132
	35241-R	CGCCGCGTCATACCATTTAC	
SeNPF	38343-F	GAACGTTTCGACACTGCTGA	130
	38343-R	CTCTGAAGATCACGGAGGCA	
vitellogenin	Vg-F	CACTCTGCCGTATCTCGCAT	130
	Vg-R	GTTGAACGTGGCTGTGAACC	
actin	Actin-F	AGGGAAATCGTGCGTGACAT	120
	Actin-R	GACCGTCGGGAAGTTCGTAG	

660

TABLE 2 Primers of partial *RyR* for clone

Gene	Prime	Squence (5'-3')
RyR	RyRs-F	GCAAGCTCAAGAGCGTATGG
	RyRs-R	CGGTAGACCTCGGAGTCATC

661
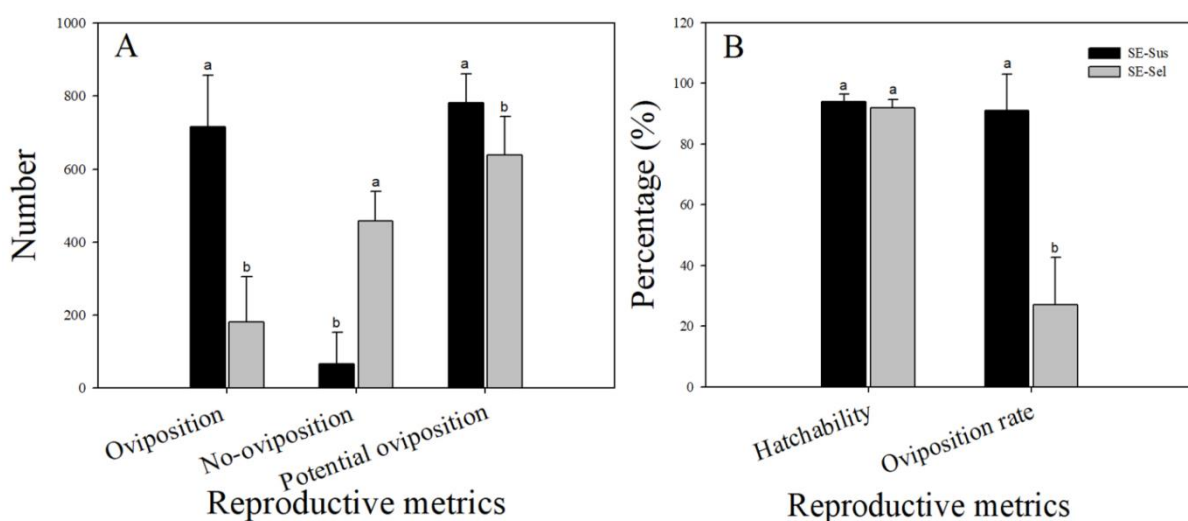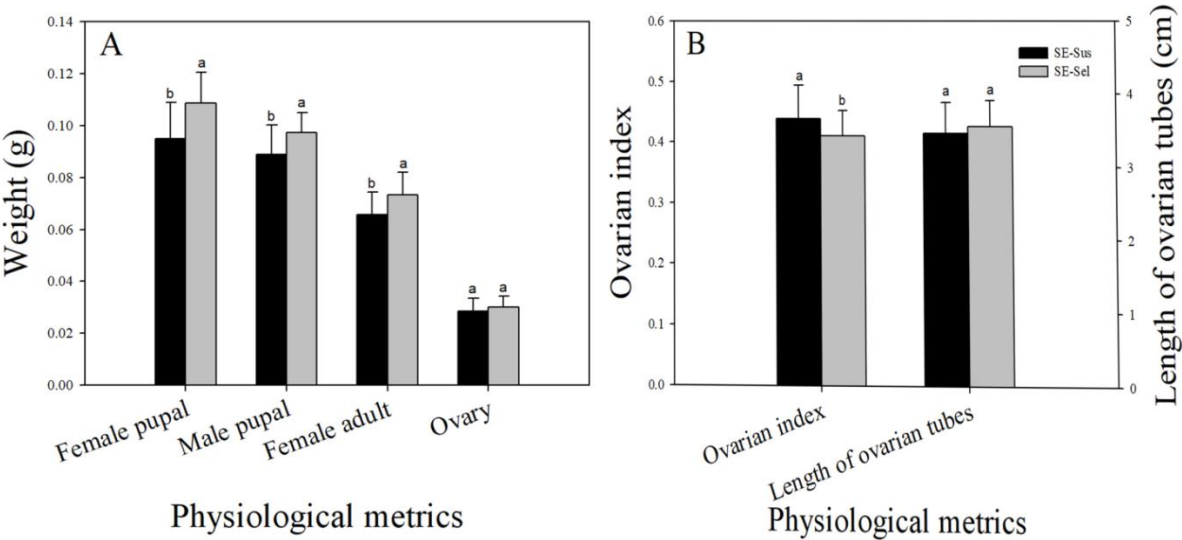662
663
664
665
666

667
668 **FIGURE 1** The Comparison and statistics of capacity between SE-Sus and SE-Sel strains. A—The

669   numbers of oviposition, no-oviposition and potential oviposition; B—The hatchability and
670   oviposition rate. Means followed by the same letters did not differ significantly ($P > 0.05$)
671   according to Duncan's multiple range test. The $F_{1, 14}$ values of different treatments on the number of
672   oviposition, no-oviposition, potential oviposition and oviposition rate of *S. exigua* were 65.324,
673   85.618, 9.277, 86.205, and the *P*-values on the numbers of oviposition, no-oviposition, potential
674   oviposition and oviposition rate of *S. exigua* were = 0.000< 0.01, = 0.000< 0.01, = 0.009< 0.01, =
675   0.000 < 0.01, respectively. While the $F_{1, 18}$ values of hatchability of SE-Sus and SE-Sel strains was
676   3.298, and the *P* values was = 0.086> 0.05.

677
678   **FIGURE 2** The comparison of physiological metrics and ovariole index between SE-Sus and SE-Sel strains.
679   A—The weight of female pupal, male pupal, female adult and ovary; B—The ovarian index and length of ovarian
680   tubes. Different letters (a, b) above bars indicate significant differences ($P < 0.05$), and means followed by the
681   same letters did not differ significantly ($P > 0.05$) according to Duncan's multiple range test. The $F_{1, 78}$ values of
682   the weight of female pupal, male pupal, female adult and ovary, the ovarian index and the length of ovarian tubes
683   of SE-Sus and SE-Sel strains were 15.703, 21.938, 16.333, 1.859, 6.517, 1.092, and the *P*-values on the weight of
684   female pupal, male pupal, female adult and ovary, the ovarian index and the length of ovarian tubes of *S. exigua*
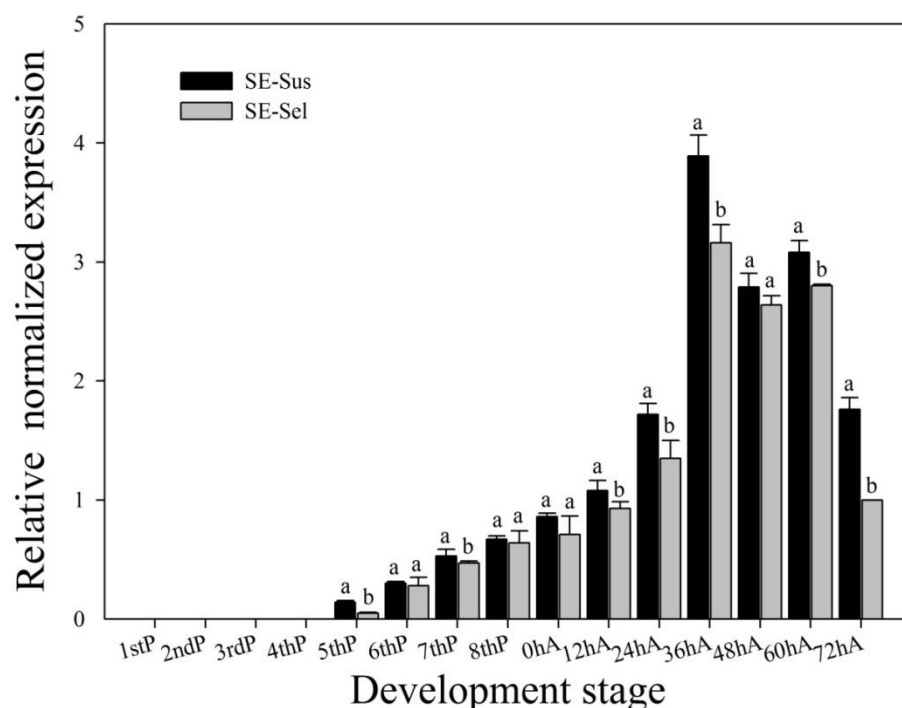685   were = 0.000< 0.01, = 0.000< 0.01, = 0.000< 0.01, = 0.177 > 0.05, = 0.013< 0.05, = 0.299 > 0.05, respectively.

686
687 **FIGURE 3** The relative normalized expression of *SeVg gene* at different development stages of in the SE-Sus and
688 SE-Sel strains. Different letters (a, b) above bars indicate significant differences ($P < 0.05$) according to Duncan's
689 multiple range test. The $F_{1, 4}$ values of the relative expression qualities of *SeVg* genes of SE-Sus and SE-Sel
690 strains at 5thP, 6thP, 7thP, 8thP, 0hA, 12hA, 24hA, 36hA, 48hA, 60hA, 72hA were 72.200, 8.977, 4.327, 2.118,
691 2.801, 10.075, 13.818, 43.361, 5.400, 47.040, 353.633, and the *P*-values on the relative expression qualities of
692 *SeVg* genes of SE-Sus and SE-Sel strains at 5thP, 6thP, 7thP, 8thP, 0hA, 12hA, 24hA, 36hA, 48hA, 60hA, 72hA
693 were =0.013 > 0.05, =0.096 > 0.05, =0.173 > 0.05, = 0.283 > 0.05, =0.170 > 0.05, =0.034 < 0.05, =0.021 < 0.05,
694 =0.003 < 0.01, =0.081 > 0.05, =0.002 < 0.01, =0.000 < 0.01, respectively.
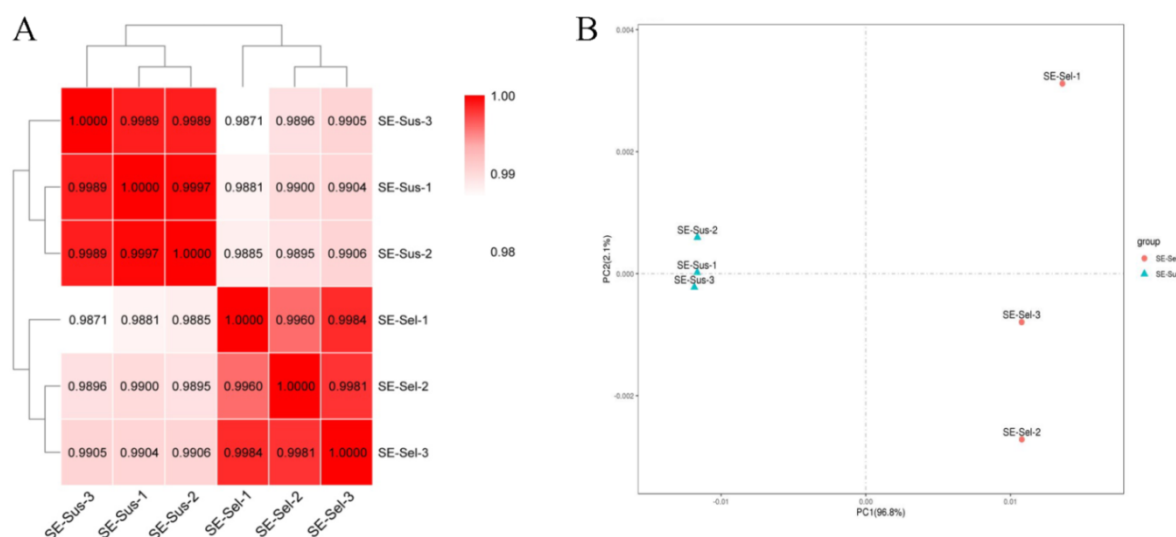

695
696 **FIGURE 4** Heat map and principal component analysis (PCA) of gene expression levels in the six samples.
697 A—Heat map; B—Principal component analysis (PCA). In the Fig. 4A, the darker the color is, the greater the
698 correlation is.

699

FIGURE 5 The statistical maps and volvano plot of DEGs among SE-Sel -vs- SE-Sus. A—The statistical maps;
B—The volvano plot. In the Fig. 5B, color-scaled represents log 2 (fold change) values for resistant lines, red
indicates up-regulated genes, green indicates down-regulated genes, and black indicates genes with no difference
in expression.

704

FIGURE 6 Bubble diagram of pathway enrichment of unigene on the different groups (Top 20). The
abscissa means KEGG terms, and the ordinate means rich factor of each term. Red color means the
terms of significant enrichment, and the bubble size indicates the number of enriched genes.

708

FIGURE 7 Gene expression pattern of the candidate genes in the SE-Sus and SE-Sel strains. A—The relative normalized expression of detoxification metabolism genes; B—The relative normalized expression of reproduction-related genes; C—The relative normalized expression of transcription factors and antimicrobial peptide genes; D—The relative nor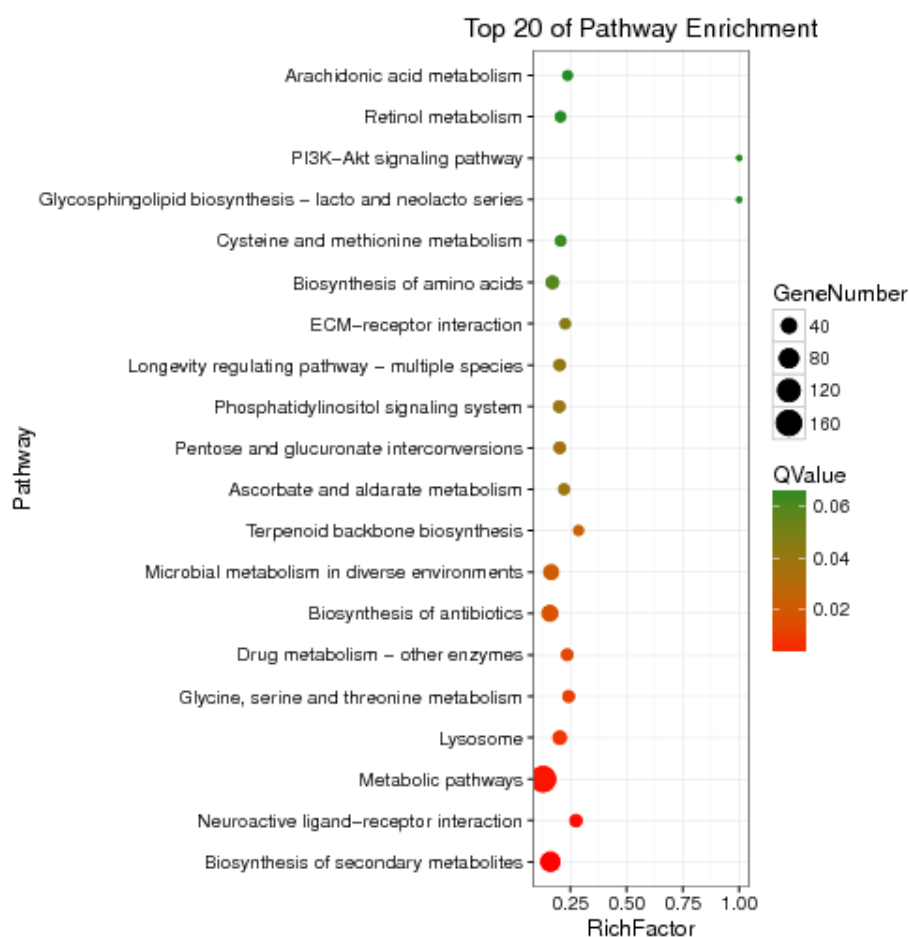malized expression of neuropeptide and sex peptide related genes. Different letters (a, b) above bars indicate significant differences ($P < 0.05$) according to Duncan's multiple range test. The $F_{1,4}$ values of the relative expression qualities of *SeABCG23*, *SeABCOK*, *SeGST15*, *SeGST1*, *SeGSTZ2*, *SeCarEs1*, *CYP6AEW*, *SeCYP6AB10*, *SeJHBWDS3*, *SeJHBAN*, *SeVgR*, *SeJHDK*, *SeSp9*, *SeTF*, *SeLE2*, *SeLE*, *SeCEB*, *SeCE*, *SeSPR*, *SeNPF* and *SeNPFR* genes of SE-Sus and SE-Sel strains were 5.458, 78.590, 229.261, 0.565, 1294.175, 201.167, 97.382, 217.622, 3194.030, 4.283, 37.569, 49.243, 25.693, 1.423, 10.630, 10.714, 141.873, 211.406, 186.483, 217.622, 1012.23, and the *P*-values on the relative expression qualities of *SeABCG23*, *SeABCOK*, *SeGST15*, *SeGST1*, *SeGSTZ2*, *SeCarEs1*, *CYP6AEW*, *SeCYP6AB10*, *SeJHBWDS3*, *SeJHBAN*, *SeVgR*, *SeJHDK*, *SeSp9*, *SeTF*, *SeLE2*, *SeLE*, *SeCEB*, *SeCE*, *SeSPR*, *SeNPF* and *SeNPFR* genes of SE-Sus and SE-Sel strains were =0.080 > 0.05, =0.001 < 0.01, =0.000 < 0.01, = 0.494 > 0.05, =0.000 < 0.01, =0.000 < 0.01, =0.001 < 0.01, =0.000 < 0.01, =0.000 < 0.01, =0.107 > 0.05, =0.009 < 0.01, =0.002 < 0.01, =0.007 < 0.01, =0.319 > 0.05, =0.031 < 0.05, =0.031 < 0.05, =0.000 < 0.01, =0.000 < 0.01, =0.000 < 0.01, =0.000 < 0.01, =0.000 < 0.01, respectively.
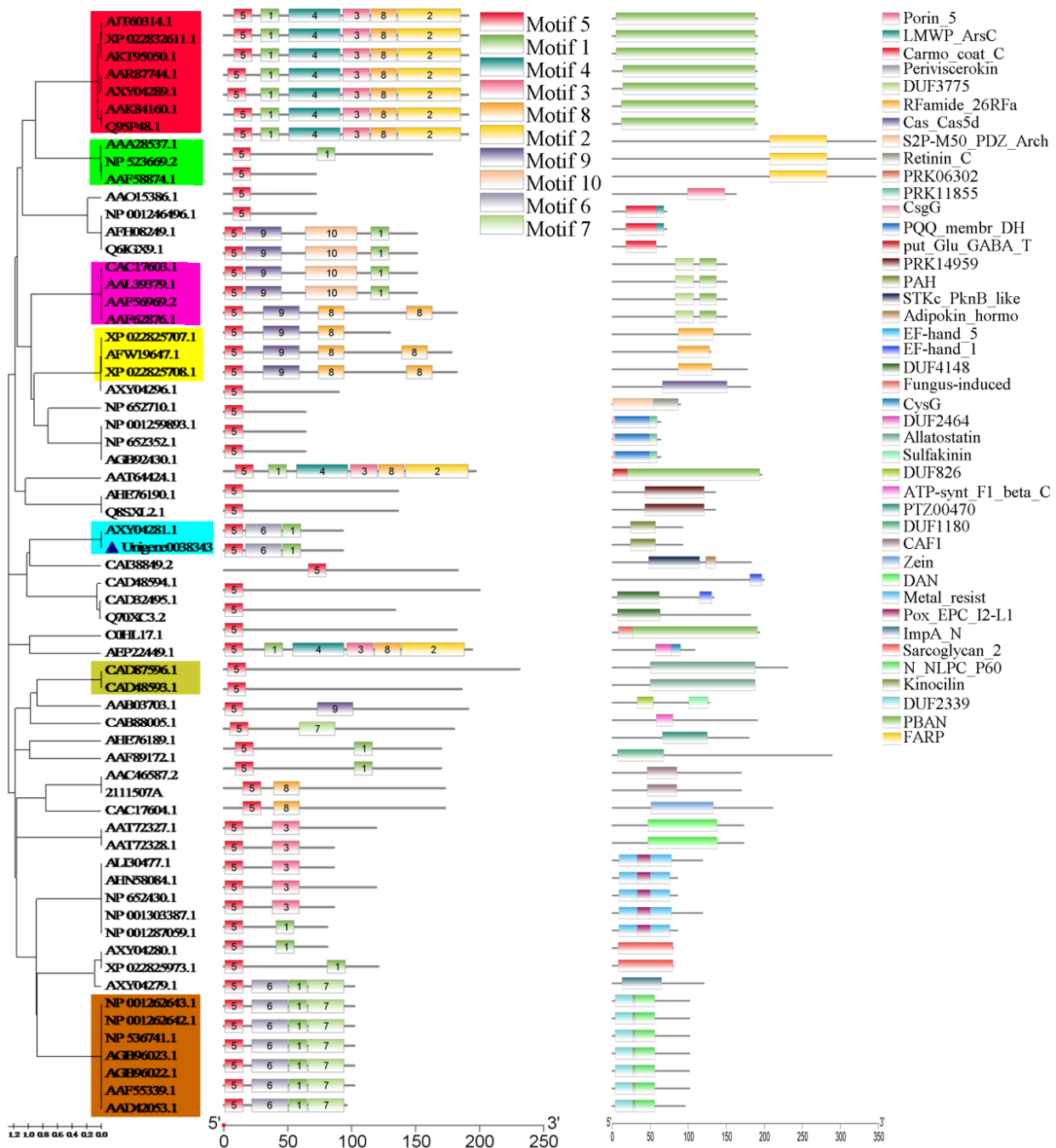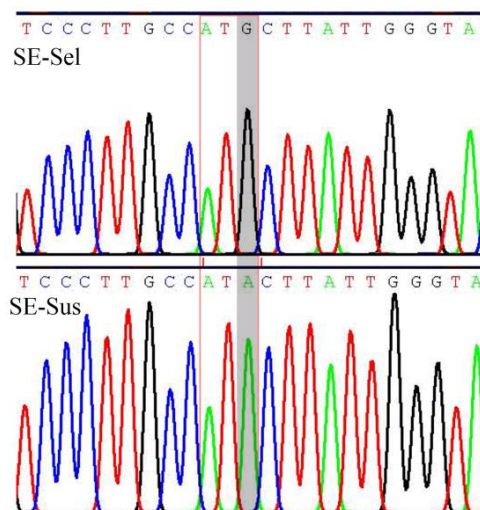
724

FIGURE 8 Phylogenetic tree of *neuropeptide* gene family constructed by NJ method and gene molecular structure map predicted by motif search and meme. In the phylogenetic tree, red-marked areas represents the PBAN family, green-marked areas represents the FMRF family; purple-marked areas represents the PBAN family with the adjunction of DUF3775 functional domains, brown-marked areas represents the neuropeptide F family in, tan-marked areas represents the Allatostatin family, blue-marked areas represents the neuropeptide Y family.

731

732   **FIGURE 9** Peak map of cloned partial sequence of RyR in SE-Sel and SE-Sus strains, the box

733   marked with black solid line indicates the mutation area, similarly hereinafter.